Journal of Alloys and Compounds 502 (2010) 488–490

Contents lists available at ScienceDirect

Journal of Alloys and Compounds

journal homepage: www.elsevier.com/locate/jallcom

# $SrFe_{12}O_{19}$/ZnO hybrid structures: Synthesis, characterization and properties

J. Jiang[a,b,*], L.H. Ai[a,b]

[a] Chemical Synthesis and Pollution Control Key Laboratory of Sichuan Province, China West Normal University, Nanchong 637002, China
[b] College of Chemistry and Chemical Engineering, China West Normal University, Shida Road 1#, Nanchong 637002, China

ARTICLE INFO

*Article history:*
Received 4 November 2009
Received in revised form 29 April 2010
Accepted 29 April 2010
Available online 5 May 2010

*Keywords:*
Hexaferrites
ZnO
Magnetic property
Hybrid structures

ABSTRACT

$SrFe_{12}O_{19}$/ZnO hybrid particles were synthesized by an in situ hydrolysis method, using zinc acetate as zinc source. X-ray diffraction (XRD), infrared spectra, scanning electron microscopy (SEM) and transmission electron microscopy (TEM) were utilized to characterize the prepared hybrid particles. The results confirmed that $SrFe_{12}O_{19}$ and ZnO coexisted in the hybrid materials. The dielectric constant and loss of $SrFe_{12}O_{19}$/ZnO hybrid particles enhanced while the saturation magnetization decreased as compared with the pure $SrFe_{12}O_{19}$.



## 1. Introduction

M-type strontium hexaferrite ($SrFe_{12}O_{19}$) is one of the most important hard magnetic materials with great scientific and technological interest. It is widely used for permanent magnets, magnetic-recording media and microwave absorbers, due to its high stability, excellent high-frequency response, large magnetocrystalline anisotropy and large magnetization as well [1].

In recent years, hybrid materials have received growing research interests, since they usually provide a new functional hybrid with synergetic or complementary activity between each constituent, which are not available from their single components, and can provide novel or enhanced properties for various applications. Especially, ferrite/metal oxide hybrid materials have attracted considerable attention because of their unique mechanical, electrical, magnetic and catalytic properties [2–5]. Recently, ZnO-based magnetic semiconductors have attracted increasing interest because of their unique properties with possible technological applications utilizing both the semiconductor physics and the ferromagnetism [6]. Thus, combining the advantages of $SrFe_{12}O_{19}$ and ZnO to fabricate a promising novel system may provide a new functional hybrid between each constituent. The prepared hybrid structures may have potential applications in magnetoelectric, magnetoiptic, spintronic devices as well as biomedical fields. However, within the limits of our knowledge, few investigations have focused on this area. More recently, we have reported the synthesis of $NiFe_2O_4$/ZnO hybrid nanoparticles with a ferromagnetic behavior [7].

In this work, herein we report the preparation of $SrFe_{12}O_{19}$/ZnO hybrid particles by the hydrolysis of zinc acetate in the presence of $SrFe_{12}O_{19}$ particles. The structural, morphological, dielectric and magnetic properties of $SrFe_{12}O_{19}$/ZnO hybrid structures were investigated.

## 2. Experimental

### 2.1. Materials

$Fe(NO_3)_3{\cdot}9H_2O$, $Sr(NO_3)_2$, $Zn(CH_3CO_2)_2{\cdot}2H_2O$, citric acid and ammonia were all analytical grade and used without further purification.

### 2.2. Preparation of $SrFe_{12}O_{19}$ particles

$SrFe_{12}O_{19}$ particles were prepared by a citrate sol–gel combustion process. Stoichiometric amounts of $Fe(NO_3)_3{\cdot}9H_2O$ and $Sr(NO_3)_2$ were dissolved in a minimum amount of deionized water by stirring on a hotplate at *ca.* 50 °C with the ratio of iron to strontium being set at 11.5. Citric acid was then added to the mixture solution to chelate $Sr^{2+}$ and $Fe^{3+}$. The molar ratios of citric acid to metal ions used were 1:1. An ammonia solution was added to adjust the pH value to 7. The clear solution was slowly evaporated at 80 °C with constant stirring and then the viscous gels were formed. By increasing the temperature to 200 °C, the dried gel precursors burnt in a self-propagating combustion manner until all the gels were burnt out completely to form brown-colored, loose powders. The entire combustion process was done in a few minutes. Finally, the as-burnt powders were calcined at 900 °C for 2 h.

### 2.3. Preparation of $SrFe_{12}O_{19}$/ZnO hybrid particles

$SrFe_{12}O_{19}$/ZnO hybrid particles were prepared by the hydrolysis of zinc acetate in the presence of $SrFe_{12}O_{19}$ particles. In a typical procedure, a certain amount of $SrFe_{12}O_{19}$ particles were dispersed in 30 mL deionized water containing 0.1 g $Zn(CH_3CO_2)_2{\cdot}2H_2O$ by ultrasonication for 30 min. 1 mol/L $NH_3{\cdot}H_2O$ was added dropwise to the above solution until pH was about 10–11, and then transferred into a

* Corresponding author at: College of Chemistry and Chemical Engineering, China West Normal University, Nanchong, Sichuan 637002, China. Tel.: +86 817 2568081; fax: +86 817 2224217.
*E-mail address:* 0826zjjh@163.com (J. Jiang).

0925-8388/$ – see front matter © 2010 Elsevier B.V. All rights reserved.
doi:10.1016/j.jallcom.2010.04.203

50 mL stainless Teflon-lined autoclave, sealed and maintained at 160 °C for 12 h, and then was cooled to room temperature naturally. The resulting product was collected by centrifugation, washed repeatedly with ethanol, and dried under vacuum at 60 °C for 24 h.

*2.4. Characterization*

X-ray diffraction patterns of the samples were collected on a Philips X'pert Pro MPD diffractometer with Cu Kα radiation (λ = 0.15418 nm). Infrared spectra were recorded on a Nicolet Avatar 360 spectrometer in the range of 400–4000 $cm^{-1}$ using KBr pellets. The compositions and SEM micrographs of samples were determined by using a Hitachi S4800 scanning electron microscope equipped with an energy dispersion spectrometer (EDS). Transmission electron microscopy (TEM) measurements were carried out on a JEOL JEM-2010 transmission electron microscope at an accelerating voltage of 200 kV. Magnetic measurements were carried out at room temperature using a vibrating sample magnetometer (VSM) with a maximum magnetic field of 15 kOe. The dielectric properties of samples at room temperature were performed on an Agilent E4991A RF Impedance/Material Analyzer in the frequency range from 1 MHz to 1 GHz.

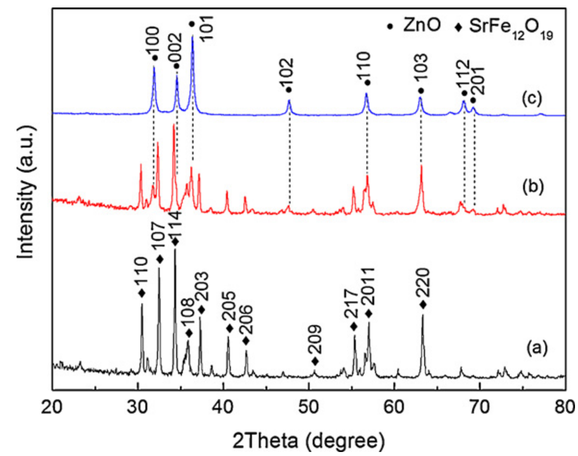


**Fig. 1.** XRD patterns of $SrFe_{12}O_{19}$ particles (a), $SrFe_{12}O_{19}$/ZnO hybrid particles (b), and ZnO (c).

## 3. Results and discussion

Fig. 1 shows the XRD patterns of the as-prepared $SrFe_{12}O_{19}$/ZnO hybrid particles. The diffraction peaks of the $SrFe_{12}O_{19}$ particles in Fig. 1(a) could be well indexed to the M-type strontium hexaferrite (JCPDS card no. 84-1531). The diffraction peaks at $2\theta$ values of 30.4, 32.4, 34.2, 35.8, 37.2, 40.4, 42.5, 50.4, 55.2, 56.9 and 63.2° can be assigned to the reflections of (1 1 0), (1 0 7), (1 1 4), (1 0 8), (2 0 3), (2 0 5), (2 0 6), (2 0 9), (2 1 7), (2 0 1 1) and (2 2 0) plans of hexagonal $SrFe_{12}O_{19}$. As shown in Fig. 1(b), besides the characteristic diffraction peaks of the $SrFe_{12}O_{19}$, the peaks at 31.8° (1 0 0), 34.4° (0 0 2), 36.3° (1 0 1), 47.6° (1 0 2), 56.6° (1 1 0), 62.8 (1 0 3), 68.1 (1 1 2) and 69.1° (2 0 1) corresponding to wurtzite phase ZnO (JCPDS card file no. 79-0206) also can be observed.

Fig. 2 shows the SEM micrographs of the as-prepared $SrFe_{12}O_{19}$/ZnO hybrid particles. As shown in Fig. 2(a), it is indicated that the $SrFe_{12}O_{19}$ particles with smooth surface appear the plate-like shape. The particle sizes of obtained $SrFe_{12}O_{19}$ are estimated to be in the range of 100–200 nm. The SEM micrograph (Fig. 2(b)) of $SrFe_{12}O_{19}$/ZnO hybrid particles is made up of irregularly shaped aggregates. The surfaces of the hybrid particles are rough, indicating that ZnO nanoparticles are attached to the surfaces of $SrFe_{12}O_{19}$ plates. TEM image of the $SrFe_{12}O_{19}$/ZnO hybrid particles shown in the inset of Fig. 2(b) indicates that plate-like $SrFe_{12}O_{19}$ particles are surrounded by ZnO nanoparticles. In addition, the EDS spectrum of $SrFe_{12}O_{19}$/ZnO particles shown in Fig. 2(c) indicates the presence of Sr, Fe, Zn and O elements.

Fig. 3 shows the FTIR spectrum of the as-prepared $SrFe_{12}O_{19}$/ZnO hybrid particles. The peaks at 601, 553 and 438 $cm^{-1}$ are assigned to the characteristic peaks of $SrFe_{12}O_{19}$. The peaks at 3440 and 1630 $cm^{-1}$ correspond to the stretching and bending modes of the hydroxyls. In addition, the characteristic band in the vicinity of 460–500 $cm^{-1}$ for ZnO is not clearly seen due to its overlapping to the characteristic peaks of $SrFe_{12}O_{19}$. Combined with the results of XRD, SEM, EDS and TEM, it can be confirmed that ZnO layers have been coated on the surfaces of $SrFe_{12}O_{19}$ particles.

Generally, dielectric response is described by the complex permittivity, where the real part ($\varepsilon'$) and imaginary part ($\varepsilon''$) represent the energy storage ability and loss ability, respectively. Fig. 4 shows the variation of dielectric constant $\varepsilon'$ and dielectric loss $\varepsilon''$ with the

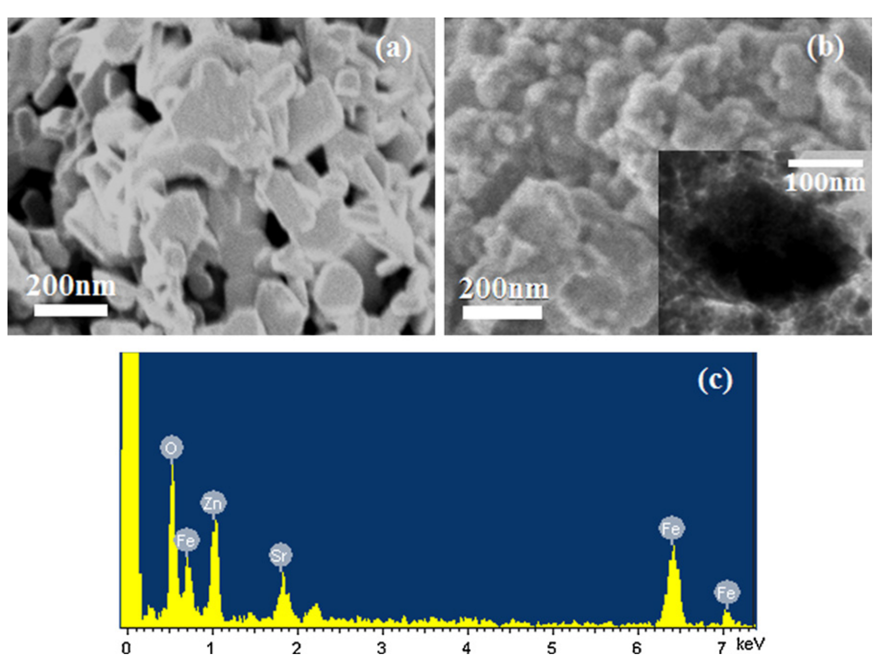


**Fig. 2.** SEM micrographs of (a) $SrFe_{12}O_{19}$ particles, (b) $SrFe_{12}O_{19}$/ZnO hybrid particles, and (c) EDS spectrum of $SrFe_{12}O_{19}$/ZnO hybrid particles. The inset is the TEM image of $SrFe_{12}O_{19}$/ZnO hybrid particles.

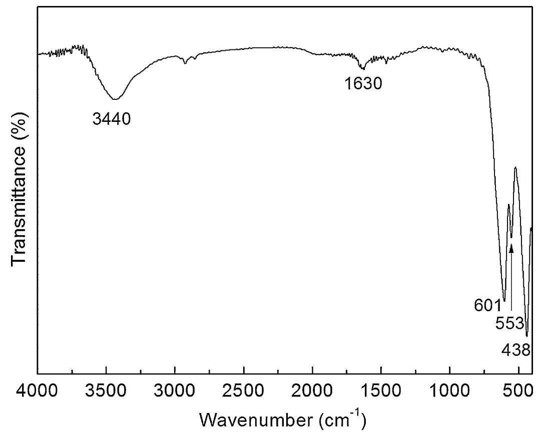


**Fig. 3.** FTIR spectrum of $SrFe_{12}O_{19}$/ZnO hybrid particles.

frequency from $10^6$ to $10^9$ Hz at room temperature for $SrFe_{12}O_{19}$ and $SrFe_{12}O_{19}$/ZnO hybrid particles. It can be clearly seen that for all samples the $\varepsilon'$ and $\varepsilon''$ decrease with increasing frequency reaching constant value at higher frequency. These observed frequency-dependent dielectric phenomena is a normal dielectric behavior of ferrites and can be explained on the basis of space charge polarization, which is a result of the presence of higher conductivity phases (grains) in the insulating matrix (grain boundaries) of a dielectric, causing localized accumulation of charge under the influence of an electric field [8,9]. Furthermore, it is noticeable that the $\varepsilon'$ and $\varepsilon''$ of $SrFe_{12}O_{19}$ are improved by coating with ZnO layer. This can be considered as follows. $SrFe_{12}O_{19}$/ZnO hybrid particles are a heterogeneous system containing magnetic particles coated with ZnO dielectric layers, may introduce an additional interfaces and more polarization charges on the surface of the particles [10,11]. The properties of interfaces between magnetic $SrFe_{12}O_{19}$ particles and ZnO dielectric layers could have a dominant role in determining dielectric performance.

Fig. 5 shows the hysteresis loops of the as-prepared $SrFe_{12}O_{19}$ and $SrFe_{12}O_{19}$/ZnO hybrid particles at room temperature. Under applied magnetic field, $SrFe_{12}O_{19}$/ZnO hybrid particles exhibit the characteristics of hard magnetic materials. It is found that the $SrFe_{12}O_{19}$/ZnO hybrid particles have a similar behavior to $SrFe_{12}O_{19}$. However, the saturation magnetization of $SrFe_{12}O_{19}$/ZnO hybrid particles is lower than that of $SrFe_{12}O_{19}$. The observed decrease in saturation magnetization reflects the standard practice of normalizing the magnetization by sample mass [12]. The nonmagnetic ZnO coating contribution to the total magnetization leads to decreasing of the saturation magnetization. Additionally, the nonmagnetic ZnO coating can be considered as a magnetically dead layer at the surface, thus affecting the uniformity or magnitude of magnetization due to quenching of surface [13,14].

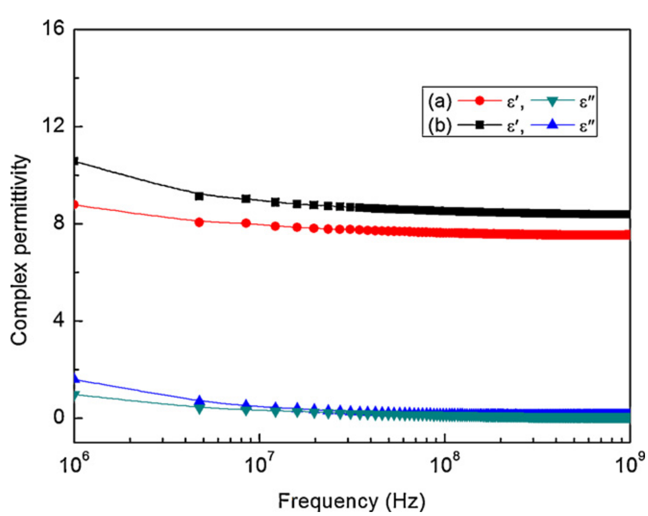


**Fig. 4.** Complex permittivity of $SrFe_{12}O_{19}$ (a) and $SrFe_{12}O_{19}$/ZnO hybrid particles (b).

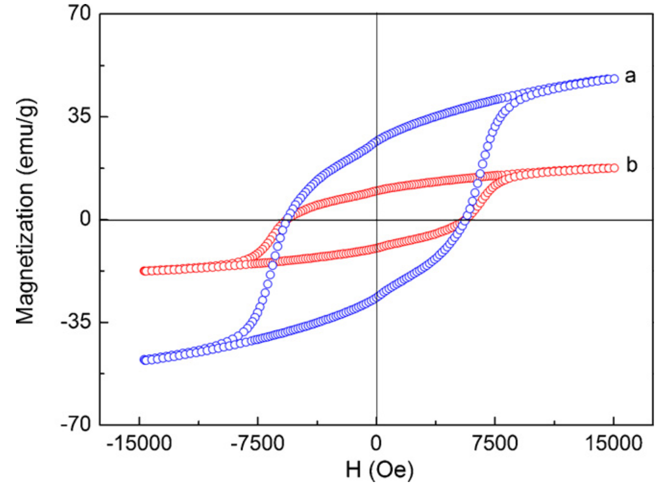


**Fig. 5.** Hysteresis loops of $SrFe_{12}O_{19}$ (a) and $SrFe_{12}O_{19}$/ZnO hybrid particles (b).

## 4. Conclusions

$SrFe_{12}O_{19}$/ZnO hybrid particles with a hard magnetic behavior were successfully synthesized by the hydrolysis of zinc acetate in the presence of $SrFe_{12}O_{19}$ particles. X-ray diffraction, infrared spectra, scanning electron microscopy and transmission electron microscopy analysis indicated the formation of $SrFe_{12}O_{19}$/ZnO hybrid particles. The dielectric constant and loss of $SrFe_{12}O_{19}$/ZnO hybrid particles enhanced due to the introduction of an additional interfaces and more polarization charges on the surface of the hybrid particles. The saturation magnetization of $SrFe_{12}O_{19}$/ZnO hybrid particles decreased as compared with the pure $SrFe_{12}O_{19}$ due to the nonmagnetic ZnO layer contribution to the total magnetization.

## Acknowledgement

This work was supported by Scientific Research Foundation of China West Normal University (07B008).

## References

[1] O. Kubo, T. Ido, H. Yok, IEEE Trans. Magn. 18 (1982) 1122–1124.
[2] T. Shinagawa, M. Izaki, H. Inui, K. Murase, Y. Awakura, Chem. Mater. 18 (2006) 763–770.
[3] R.K. Selvan, V. Krishnan, C.O. Augustin, H. Bertagnolli, C.S. Kim, A. Gedanken, Chem. Mater. 20 (2008) 429–439.
[4] M. Artus, S. Ammar, L. Sicard, J.Y. Piquemal, F. Herbst, M.J. Vaulay, F. Fievet, V. Richard, Chem. Mater. 20 (2008) 4861–4872.
[5] Y. Zhang, F. Zhang, Y. Lu, T. Chen, L. Yang, J. Phys. Chem. Solids 71 (2010) 604–607.
[6] R.K. Singhal, A. Samariya, Y.T. Xing, S. Kumar, S.N. Dolia, U.P. Deshpande, T. Shripathi, E.B. Saitovitch, J. Alloys Compd. 496 (2010) 324–330.
[7] J. Jiang, L.-H. Ai, L.-C. Li, J. Alloy Compd. 484 (2009) 69–72.
[8] M.C. Dimri, S.C. Kashyap, D.C. Dube, Ceram. Int. 30 (2004) 1623–1626.
[9] H. Zhang, Z. Liu, C. Ma, X. Yao, L. Zhang, M. Wu, Mater. Chem. Phys. 80 (2003) 129–134.
[10] J. Cao, W. Fu, H. Yang, Q. Yu, Y. Zhang, S. Liu, P. Sun, X. Zhou, Y. Leng, S. Wang, B. Liu, G. Zou, J. Phys. Chem. B 113 (2009) 4642–4647.
[11] X. Tang, B.Y. Zhao, Q. Tian, K.A. Hu, J. Phys. Chem. Solids 67 (2006) 2442–2447.
[12] C.R. Vestal, Z.J. Zhang, Nano Lett. 3 (2003) 1739–1743.
[13] S. Rana, J. Rawat, R.D.K. Misra, Acta Biomater. 1 (2005) 691–703.
[14] K.H. Wu, T.H. Ting, G.P. Wang, C.C. Yang, B.R. McGarvey, Mater. Res. Bull. 40 (2005) 2080–2088.